Rotational diffusion of a steroid molecule in phosphatidylcholine membranes: Effects of alkyl chain length, unsaturation, and cholesterol as studied by a spin-label method

ARTICLE *in* BIOCHEMISTRY · JULY 1988

Impact Factor: 3.02 · DOI: 10.1021/bi00412a030 · Source: PubMed

2 AUTHORS, INCLUDING:

Marta Pasenkiewicz-Gierula
Jagiellonian University
88 PUBLICATIONS **2,740** CITATIONS

SEE PROFILE

Rotational Diffusion of a Steroid Molecule in Phosphatidylcholine Membranes: Effects of Alkyl Chain Length, Unsaturation, and Cholesterol As Studied by a Spin-Label Method†

Akihiro Kusumi*

Microphotonic Center, Department of Radiology, Medical College of Wisconsin, Milwaukee, Wisconsin 53226, and Department of Biophysics, Faculty of Science, Kyoto University, Kyoto 606, Japan

Marta Pasenkiewicz-Gierula

National Biomedical ESR Center, Department of Radiology, Medical College of Wisconsin, Milwaukee, Wisconsin 53226, and Biophysics Department, Institute of Molecular Biology, Jagiellonian University, Krakow, Poland

Received September 10, 1987; Revised Manuscript Received January 11, 1988

ABSTRACT: Rotational diffusion of cholestane spin-label (CSL), a sterol analogue, in various phosphatidylcholine (PC)–cholesterol membranes was systematically studied by computer simulation of steady-state ESR spectra as a function of chain length and unsaturation of alkyl chains, cholesterol mole fraction, and temperature for better understanding of phospholipid–cholesterol and cholesterol–cholesterol interactions. CSL motion in the membrane was treated as Brownian rotational diffusion of a rigid rod within the confines of a cone imposed by the membrane environment. The wobbling rotational diffusion constant of the long axis, its activaton energy, and the cone angle of the confines are obtained for various membranes in the liquid-crystalline phase. The wobbling diffusion constant decreases in the order dilauroyl-PC > dimyristoyl-PC > dioleoyl-PC ~ dipalmitoyl-PC > distearoyl-PC > dioleoyl-PC/cholesterol = 3/1 > dioleoyl-PC/cholesterol = 1/1 membranes. Activation energy for the wobbling diffusion of the long axis of CSL is strongly dependent on alkyl chain length, unsaturation, and cholesterol mole fraction. It decreases with decrease in alkyl chain length and by introduction of unsaturation in the alkyl chains. In dioleoylphosphatidylcholine membranes, activation energy decreases by a factor of ~3 in the presence of 50 mol % cholesterol. Activation energy for wobbling diffusion of CSL in phosphatidylcholine membranes is smaller than the activation energy for translational diffusion of a phospholipid. The former is more dependent on alkyl chain length and unsaturation. The cone angle decreases in the order dilauroyl-PC > dioleoyl-PC > dimyristoyl-PC > dioleoyl-PC/cholesterol = 3/1 > dipalmitoyl-PC > distearoyl-PC ≫ dioleoyl-PC/cholesterol = 1/1 membranes. The importance of simultaneous evaluation of the rotational diffusion constant and the restoring potential (cone angle) imposed by the membrane environment is clearly shown.

Liposomes and reconstituted membranes made of phosphatidylcholine (PC)[1] or PC/cholesterol have been extensively utilized to study biochemical and biophysical processes involving biological membranes. Recent studies include examination of protein–lipid interactions in reconstituted membrane vesicles (Kusumi et al., 1980; Dempsey et al., 1986; Arderle & Mendelsohn, 1986), observation of PC membrane disruption by adenovirus (Blumenthal et al., 1986), and measurement of rate and extent of poly(ethylene glycol)-induced membrane fusion using large unilamellar PC vesicles (Parente & Lentz, 1986). For further advancement of these types of studies, more comprehensive understanding of lipid organization and mobilities in the membrane is necessary. Recently, we have been systematically studying the effects of alkyl chain length, unsaturation, and cholesterol mole fraction on membrane structure, lipid mobilities, and membrane protein association by using various spin-labeling techniques and time-resolved fluorescence methods. The following are key findings of this series of studies.

(1) Transient dimers and oligomers of rhodopsin are frequently formed in both disk membranes and reconstituted membranes. The dimensional mismatch between the hydrophobic domains of rhodopsin and the thickness of the membrane (alkyl chain length of lipids) increases the extent of rhodopsin association (Kusumi & Hyde, 1982).

(2) The oxygen transport parameter (Kusumi et al., 1982) and the copper complex transport parameter (Subczynski et al., 1987) in the membrane are very strongly affected by the presence of cholesterol in saturated PC membranes (Subczynski et al., 1988).

(3) Incorporation of cholesterol decreases motional freedom of alkyl chains in saturated PC membranes. Unsaturation of alkyl chains moderates the effect of cholesterol (Kusumi et al., 1986; Merkle et al., 1987).

(4) Incorporation of cholesterol increases the rotational diffusion rate of band 3, erythrocyte anion channel protein, in saturated PC [dimyristoylphosphatidylcholine (DMPC)] reconstituted membranes, but decreases the rate in unsaturated PC [dioleoylphosphatidylcholine (DOPC)] reconstituted membranes (A. Kusumi, A. Tsuji, W. K. Subczynski, and S. Ohnishi, unpublished results).

†This work was supported in part by U.S. Public Health Service Grants GM22923 and RR01008 and by Grant-in-Aid 61302085 from the Ministry of Education, Science, and Culture of Japan.

*Address correspondence to A.K. at the Department of Pure and Applied Sciences, College of Arts and Sciences, The University of Tokyo, Meguro-ku, Tokyo 153, Japan.

[1] Abbreviations: PC, phosphatidylcholine; DLPC, L-α-dilauroylphosphatidylcholine; DMPC, L-α-dimyristoylphosphatidylcholine; DPPC, L-α-dipalmitoylphosphatidylcholine; DSPC, L-α-distearoylphosphatidylcholine; DOPC, L-α-dioleoylphosphatidylcholine; CSL, cholestane spin-label; HEPES, 4-(2-hydroxyethyl)-1-piperazineethanesulfonic acid.

0006-2960/88/0427-4407$01.50/0

(5) Incorporation of cholesterol in DMPC membranes decreases the lateral diffusion constant of a fluorescently labeled phosphatidylethanolamine, *N*-(7-nitro-2,1,3-benzoxadiazol-4-yl)dipalmitoyl-L-α-phosphatidylethanolamine. However, the presence of cholesterol gives little effect on lateral diffusion in DOPC membranes (Kusumi et al., 1986).

In the present work, we have extended this line of research to study the effects of alkyl chain length, unsaturation, and incorporation of cholesterol on the rotational diffusion of cholestane spin-label (CSL), a sterol analogue.

Two primary reasons for the use of CSL, a spin-labeled sterol analogue, are the following: (1) CSL facilitates the study of phospholipid–cholesterol and cholesterol–cholesterol interactions (Presti & Chan, 1982; Presti et al., 1982). CSL has been shown to behave in a way very similar to that of cholesterol in membranes formed at air–water interface (Müller-Landau & Cadenhead, 1979a,b; Cadenhead & Müller-Landau, 1979) or in liposomes (Kusumi et al., 1986). (2) CSL makes it possible to obtain both the rotational diffusion constant (which can be related to "viscosity" of the local environment) of this molecule and the restoring potential on this molecule imposed by the membrane structure (order parameter in a true sense). Since the core part of CSL shows little intramolecular motion due to its rather rigid structure, it is possible to obtain both of these physical parameters. Very large intramolecular mobility (gauche–trans isomerization of alkyl chains) of other commonly used lipid spin probes such as stearic acid spin-labels and phospholipid labels prevents one from obtaining the rotational diffusion constant of the probe molecule as a whole.

Recently, Dufourc and Smith (1986) made NMR relaxation studies on cholesterol motion in the membrane and described both order and the rates of motion separately. We also emphasize the importance of separate evaluation of the rotational diffusion constant of CSL (which can be related to viscosity) and the restoring potential on CSL imposed by the membrane structure. These two concepts are often confused in the literature, especially in interpretation of spectral order parameters obtained by ESR, NMR, or steady-state fluorescence methods.

The order parameter (S) of lipid alkyl chains in the membrane can be expressed as

$$S = [(3\cos^2\theta - 1)/2]_{av} \quad (1)$$

which is a measure of the average wobbling angle of the long axis of the lipid molecule with respect to the membrane normal (θ). If the average in (1) is an ensemble average, the order parameter is then a measure of restoring potential in the membrane. However, in the case when parameter S is obtained by spectroscopic methods, the average in (1) is often not an ensemble average but a time average over a characteristic time scale associated with the spectroscopic technique (McConnell, 1976). In this case, eq 1 has some meaning only if it is considered with the time scale during which the average in the above equation takes place. In the case of ESR spectroscopy of nitroxide spin-labels, the time scale is of the order of anisotropic hyperfine interaction between the electron and the nitrogen nucleus (10^{-8} s), and in the case of deuterium magnetic resonance, it is of the order of anisotropic quadrupole interaction between deuterium nuclei (10^{-5} s). Therefore, the identical motion is likely to be described by different order parameters if different spectroscopic methods are used to study it (McConnell, 1976).

To describe the rotatonal diffusion of CSL and the restoring potential in the membrane, we adopted Brownian diffusion within a cone (half-cone angle = θ_c) as a simple model (Hemminga, 1974, 1977; Israelachvili et al., 1975; Griffith & Jost, 1976). This approach is similar to the method used to analyze time-resolved (or phase modulation) fluorescence depolarization decay data (Kawato et al., 1977, 1978; Kinosita et al., 1977; Engel & Prendergast, 1981). The computer program used to simulate ESR spectra of CSL in the membrane is based on the theory developed by Jost and Griffith (1973), Mailer et al. (1974), and Israelachvili et al. (1975). From the half-cone angle and the rotational correlation time obtained by spectral simulation, the diffusion constant was calculated according to the theory of Wang and Pecora (1980).

We systematically studied PC membranes in the liquid-crystalline phase by varying the chain length [dilauroyl-PC (DLPC), dimyristoyl-PC (DMPC), dipalmitoyl-PC (DPPC), and distearoyl-PC (DSPC)], unsaturation (DOPC), cholesterol content, and temperature.

Outline of Theory. CSL motion in the membrane is treated as Brownian rotational diffusion of a rigid rod within the confines of a cone of a semicone angle of θ_c. These spatial confines imposed by the environment (restoring potential) can be described as a square well potential with infinitely high barriers at $\pm\theta_c$ (which may approximate a Gaussian shape of the potential). In this model, one considers two *independent* modes of CSL motion: (1) axial rotation of CSL, i.e., CSL rotates rapidly about its long axis, irrespective of the orientation of the long axis; and (2) wobbling of the long axis itself, i.e., CSL (rigid rod) reorients rapidly with a diffusion constant D_w within the confines of a cone of a semicone angle of θ_c. Diffusion of a rod may be described by the diffusion equation

$$\frac{\partial\psi(\hat{u},t)}{\partial t} = D_w\frac{1}{\sin^2\theta}\left[\sin\theta\frac{\partial}{\partial\theta}\left(\sin\theta\frac{\partial}{\partial\theta}\right) + \frac{\partial^2}{\partial\phi^2}\right]\psi(\hat{u},t) \quad (2)$$

where $\psi(\hat{u},t)$ is the probability density for finding the rod (long axis of CSL) oriented in the direction of $\hat{u}$ (unit vector) at time t. The viscosity in the cone is reflected in D_w.

To simulate ESR spectra of CSL in the membrane, the method of Israelachvili et al. (1975) was used with the following assumptions: (1) The motion in the cone is so fast that the resonant field position can be calculated by effective Hamiltonian approach [for the mathematical expression, see Israelachvili et al. (1975), eq 11] and the rotational diffusion about its long axis is not restricted (meaning $\phi = 90°$). (2) The line width is dependent on motion and expressed as

$$\Gamma_m = \Gamma_r + \left(\frac{h\nu}{\beta_e g_0^2}\Delta g + m\Delta T\right)^2(\langle\cos^4\theta\rangle - \langle\cos^2\theta\rangle^2)\,\gamma_e\tau_w + \tfrac{1}{8}\left(\frac{h\nu}{\beta_e g_0^2}\delta g + m\delta T\right)^2\langle\sin^4\theta\rangle\,\gamma_e\tau_R \quad (3)$$

where Γ_r is the residual line width, β_e is the Bohr magneton, γ_e is the magnetogyric ratio of free electron, τ_w and τ_R are rotational correlation times, and

$$g_0 = \tfrac{1}{3}(g_x + g_y + g_z)$$
$$\Delta g = g_y - \tfrac{1}{2}(g_z + g_x)$$
$$\Delta T = T_y - \tfrac{1}{2}(T_z + T_x) \quad (4)$$
$$\delta g = g_x - g_z$$
$$\delta T = T_x - T_z$$

$\langle\cos^4\theta\rangle - \langle\cos^2\theta\rangle^2$ and $\langle\sin^4\theta\rangle$ depend on θ_c and the angle between the cone axis and the magnetic field. The correlation time τ_R appearing in the third term of eq 3 arises from both

axial rotation and wobbling. Therefore, τ_R represents a mixed correlation time of rotation and wobbling (Israelachvili et al., 1975). τ_R of different samples can be compared only when the cone angle is the same. The other correlation time, τ_w, appearing in the second term of eq 3 arises from pure wobbling within the cone. Therefore, τ_w represents the wobbling correlation time (Israelachvili et al., 1975).

D_w in eq 2 may be related to τ_w and θ_c according to the theory of Wang and Pecora [eq 55 and 74 (1980)]

$$\langle Y_{2,0}(\hat{u}(0))Y_{2,0}^*(\hat{u}(t))\rangle = \frac{5}{4\pi}\sum_{n=1}^{\infty} C_n^0 \exp[-\nu_n^0(\nu_n^0 + 1)D_w t] \sim \frac{5}{4\pi}(C_1^0 + C_2^0 \exp[-\nu_2^0(\nu_2^0 + 1)D_w t] \quad (5)$$

$$D_w = 1/[\nu_2^0(\nu_2^0 + 1)\tau_w] \quad (6)$$

ν_2^0 is a function of the cone angle and calculated according to the method of Pal (1918). According to eq 6, the wobbling rotational correlation time, τ_w, depends on both diffusion constant and cone angle. Since the cone angle and τ_w can be obtained by spectral simulation, we can evaluate the diffusion constant, D_w.

Experimental Procedures

Sample Preparation. CSL was obtained from Syva (Palo Alto, CA). All phospholipids were purchased from Sigma (St. Louis, MO) and cholesterol (crystallized) from Boehringer (Indianapolis, IN). All reagents were used without further purification. Lipids and CSL were mixed at a molar ratio of 400:1 in chloroform, and the solvent was evaporated with a stream of nitrogen gas. Residual lipids were placed under vacuum (~0.06 mmHg) for at least 12 h. Liposomes (multilamellar dispersion of lipids) were formed by adding 65 mM NaCl buffered with 10 mM HEPES (pH 7.6) to dried lipid at temperatures 25 °C above the phase-transition temperature of each phospholipid and vortexing. Liposomes were centrifuged at 12800*g* for 10 min at 4 °C, and the loose pellet was used for ESR measurements.

ESR Measurements of CSL—Fast Motional Case. All samples were deoxygenated by placing them in a gas-permeable capillary (i.d. 0.7 mm) made from a methylpentene polymer called TPX (Popp & Hyde, 1980). This plastic is permeable to oxygen, nitrogen, and carbon dioxide and is substantially impermeable to water. Samples were equilibrated with nitrogen gas that was used for temperature control.

ESR spectra of CSL undergoing fast motion were obtained with a Varian E-109 X-band spectrometer with a Varian variable-temperature accessory and an E-231 Varian multipurpose cavity (rectangular TE_{102} mode). The same Dewar insert was used to maintain a constant effective microwave filed on the sample throughout this study (Kusumi et al., 1978, 1980). Modulation width (peak-to-peak) of 0.5 G and incident microwave power of 0.5 mW were used. Although this power is much less than the power level employed conventionally, we observed very slight saturation of ESR signal. Nevertheless, 0.5 mW was utilized to improve the signal-to-noise ratio.

ESR Measurements of Rigid-Limit Spectra at Q-band. Q-band spectra were recorded with a Varian E-110 microwave bridge connected to a Varian E-9 spectrometer with a Varian variable-temperature accessory and a Varian cylindrical cavity (TE_{011} mode). For second-derivative display, a field modulation of 50 kHz with in-phase detection at 100 kHz was used.

Simulation of ESR Spectra. (a) Determination of Magnetic Parameters of CSL in Various PC Membranes. Since the magnetic parameters of CSL in membranes are strongly dependent on PC species and cholesterol content of host membranes (Kusumi et al., 1986), we determined them for each PC–cholesterol membrane. To suppress the motional effect, the membrane suspension was cooled to −120 °C (Griffith & Jost, 1976). The validity of using these parameters to simulate ESR spectra for rapid motional cases at higher temperatures (0–80 °C) will be given under Results and Discussion.

First, A_z and g_z for CSL were determined experimentally from the X-band ESR spectrum recorded at −120 °C for each membrane. The microwave frequency was measured with a frequency counter (EiP Model 331). The magnetic field was calibrated both with a gaussmeter (Radiopan MJ-110R) and against standard samples: 0.1 mM solution of Fremy's salt ($g = 2.005\,50 \pm 0.000\,05$, $2A_0 = 26.182$ G) and manganese in SrO (a hyperfine splitting value of 84.0 G) (Borg, 1972).

Determination of other magnetic parameters was carried out by simulating Q-band second-derivative ESR spectra at −120 °C. Because second-derivative Q-band spectra are richer in spectral features compared with conventional first-derivative X-band spectrum at the rigid limit, more precise simulation is possible in this display. Nevertheless, experimental determination of A_z can be carried out more precisely at X-band because $2A_z$ can be measured at high signal-to-noise ratio.

Simulation of rigid-limit Q-band spectra was carried out as described by Pasenkiewicz-Gierula et al. (1983). Briefly, resonant field positions were calculated for 2100 different orientations of magnetization. Each resonant line was assumed to possess Gaussian line shape. This calculation was carried out for different nuclear states of the nitrogen atom ($m = 1$, 0, −1), and resultant lines were superimposed to obtain a spectrum. Central processing unit time for simulation was about 20 min on a DEC PDP 11-34 minicomputer equipped with a floating point processor.

(b) Rapid Motional Spectra at X-band. The ESR line shape of CSL undergoing rapid motion is a combination of Lorentzian and Gaussian functions. We assumed that Gaussian characteristics of the line shape result from a binomial distribution of Lorentzian lines (line shape of each spin packet) due to the superhyperfine interaction with methyl protons. Thus, we first calculated the spectrum by using Lorentzian line shape and then carried out a Gaussian "post-broadening" (Rao et al., 1977) with the half-width of 0.97 G. This number corresponds to an interaction with 10 protons with the same isotropic superhyperfine splitting value of 0.65 G. The value of 0.97 G is the upper limit that allowed us to simulate every spectrum in this work, and we kept it constant. The change in the ratio of Gaussian broadening width and Lorentzian residual width (related to T_2) did not affect motional and structural parameters such as θ_c, τ_R, and τ_w if the sum of the two line widths is the same.

Spectral simulation was achieved by the following procedure: (1) Determine the residual width (Lorentzian) from the central region ($m = 0$) of the spectrum, keeping it as small as possible. (2) Vary the cone angle until the positions of high- and low-field peaks match those of experimental lines. (3) Vary τ_R and τ_w to obtain proper line widths for all lines ($m = +1$, 0, −1). τ_R affects central- and high-field regions of the spectrum more than low-field regions, while τ_w affects low-field regions most. (4) Readjust the Lorentzian residual line width and the cone angle because changes in τ_R and τ_w cause changes in line width of the central peak and crossover points of high- and low-field lines across the base line.

The central processing unit time to simulate fast motional spectra was between 1.5 and 3 min on a DEC PDP 11-34

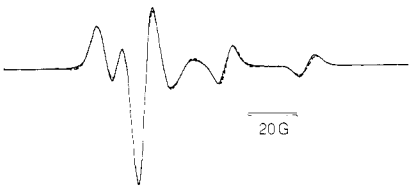

FIGURE 1: Experimental (solid line) and simulated (broken line) second-derivative Q-band ESR spectra of CSL in DOPC membranes at −120 °C.

Table I: Magnetic Parameters of CSL in Various PC Membranes

host lipid	g_x	g_y	g_z[a]	A_x (G)	A_y (G)	A_z[a] (G)
DLPC	2.008 53	2.006 00	2.002 31	5.4	5.0	33.8
DMPC	2.008 61	2.006 05	2.002 29	6.1	5.0	34.0
DPPC	2.008 57	2.005 98	2.002 29	5.0	4.9	34.0
DSPC	2.008 81	2.006 22	2.002 32	6.2	4.6	33.2
DOPC	2.008 80	2.006 19	2.002 29	5.9	4.8	33.1
DOPC/chol[b]						
=3/1	2.008 51	2.005 98	2.002 28	5.2	4.9	34.7
=1/1	2.008 40	2.005 93	2.002 26	5.2	4.9	35.0

[a] g_z and A_z were obtained experimentally. [b] chol indicates cholesterol.

minicomputer and about 10 s on a Masscomp microcomputer.

Results and Discussion

Determination of Magnetic Parameters of CSL in Various Phosphatidylcholine Membranes. A number of methods for analysis of ESR spectra of CSL in membranes and liquid crystals have been published (Jost & Griffith, 1973; Mailer et al., 1974; Schindler & Seelig, 1974; Israelachvili et al., 1975; Shimoyama et al., 1978; Polnaszek et al., 1981). However, in none of them were the magnetic parameters (g and A tensors) of CSL determined in membranes. We found it necessary to use magnetic parameters determined in situ rather than those determined in single crystals. This is probably due to the fact that the environment around the nitroxide radical in the membrane is very different from that in single crystals. Moreover, the magnetic parameters are dependent on the host lipid. Figure 1 shows the experimental and simulated second-derivative spectra of CSL at Q-band at −120 °C. Further lowering of the temperature did not change the peak position, and the mobility of CSL was regarded to be almost frozen in the time scale of anisotropy of nitroxide radical at this temperature. Pasenkiewicz-Gierula et al. (1983) showed that a Q-band second-derivative spectrum is a favorable display for determination of all six magnetic parameters. They were able to determine g- and A-values of nitroxide spin-labels more accurately by using frozen solutions rather than by using single crystals as performed before. They noticed deterioration of fit for changes of ±0.00002 in g-values and ±0.2 G in A-values. Kusumi et al. (1986) determined magnetic parameters for CSL in several PC and PC–cholesterol membranes and found that the magnetic parameters of CSL are dependent on PC alkyl chains and cholesterol content. These parameters reflect the polarity of the membrane surface around the nitroxide group of CSL and are sensitive to an increase of water accessibility to the membrane surface induced by incorporation of cholesterol. Thus, in order to simulate rapid motional spectra of CSL in various lipids, it is necessary to determine the magnetic parameters in each PC (PC–cholesterol) membranes. These magnetic parameters are listed in Table I. Estimated accuracy of g values and A-values was about ±0.000 05 and ±0.25 G, respectively. These values were used for simulation of fast motional spectra. Since we were able to simulate ESR spectra of CSL undergoing rapid motion using the magnetic parameters determined for each PC (PC–cholesterol) membrane at −120 °C and since we obtained unsatisfactory fit for CSL undergoing rapid motion when we used magnetic parameters determined in different host lipid membranes or those determined on the basis of single-crystal studies (Hubbell & McConnell, 1971; Goldman et al., 1972; Schindler & Seelig, 1973), the magnetic parameters determined by freezing the liposome suspension seem to be proper for simulating fast motional spectra of CSL, and the differences in magnetic paramers for various host lipids are significant.

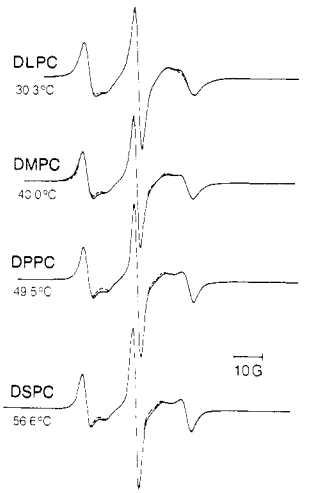

FIGURE 2: Experimental (solid line) and simulated (broken line) X-band ESR spectra of CSL in various saturated PC membranes. Temperature is adjusted so that the overall splitting values become approximately the same for easy comparison of line widths.

Mobility of CSL in PC Membranes with Various Alkyl Chain Lengths. Figure 2 shows several experimental and simulated X-band spectra of rapidly moving CSL in membranes. These spectra were selected to show samples with different line shapes but equal overall splitting values. The fit was good for spectra taken above the phase-transition temperature. We were unable to satisfactorily simulate spectra taken around and below the phase-transition temperature because the assumption of rapid motion is not satisfied. In subsequent figures, points shown in parentheses indicate the temperature region where the fit becomes less satisfactory.

Estimation of the accuracy of motional and structural parameters is difficult to determine. However, (1) changes in the cone angle by more than 2° or (2) changes in τ_R by ~15% lead to an obviously worse fit. (3) Simulation is very sensitive to τ_w, especially when τ_w is smaller than 0.7 ns. (4) It is impossible to satisfactorily simulate the spectrum for rapid motion when magnetic parameters for CSL in different host lipid membranes are used.

The fit between simulated and experimental spectra is poor below and around the phase-transition temperature of each phospholipid. This shows a limitation of the theory employed in this work. An attempt was made to use computer programs based on the stochastic Liouville theory developed by Freed's group (Polnaszek et al., 1973, 1981; Meirovitch & Freed, 1983). However, when restoring potential was included in the program, computation time was inhibitively long even for CSL undergoing rapid motion. When the restoring potential was removed from the program, it was impossible to satisfactorily simulate CSL spectra in membranes.

The Lorentzian residual line width (half width at half height) is plotted against temperature in Figure 3. For lipids used in this work, all points follow the same curve except those measured below the phase-transition temperatures. The range of spin–spin relaxation time calculated from the residual line

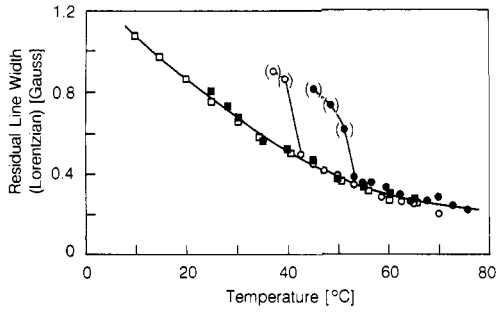

FIGURE 3: Lorentzian residual line width of CSL in various PC membranes plotted against temperature: (□) DLPC; (■) DMPC; (○) DPPC; (●) DSPC.

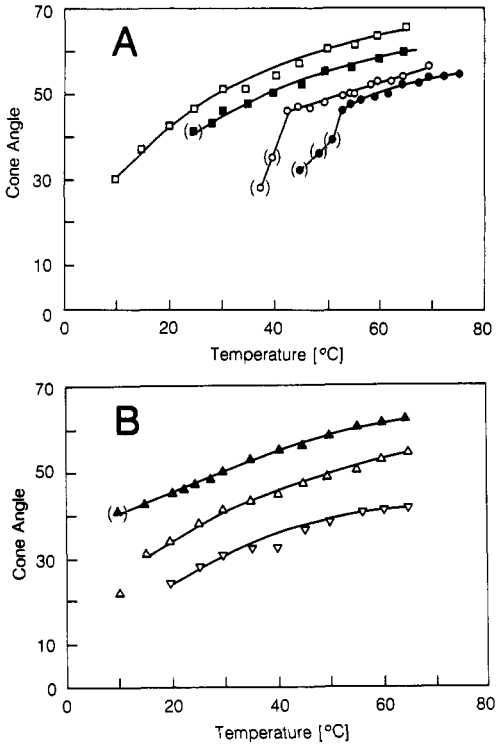

FIGURE 4: Semicone angle of CSL motion plotted against temperature in saturated PC (A) and DOPC–cholesterol (B) membranes. (A) (□) DLPC; (■) DMPC; (○) DPPC; (●) DSPC. (B) (▲) DOPC; (△) DOPC/cholesterol = 3/1; (▽) DOPC/cholesterol = 1/1.

width is between 5.3×10^{-8} (10 °C) and 2.5×10^{-7} s (76 °C), which is in general agreement with the transverse relaxation times for CSL in egg-yolk PC membranes obtained by the electron spin–echo method by Madden et al. (1980).

The cone angle is plotted as a function of temperature in Figure 4. The cone angle decreases with increase in the alkyl chain length at a given temperature. This result is to be compared with the ESR spin-labeling data on motion of fatty acid spin-labels (5- and 16-doxylstearic acid) in PC membranes with various alkyl chain length (Kusumi et al., 1986): the mobility of 5- and 16-doxylstearic acid does not depend on alkyl chain length of the host PC except for DLPC. Because of the rigid fused-ring system of CSL, CSL motion may be sensitive to the overall order along the host alkyl chain, while the stearic acid spin-labels may be sensitive to local motional freedom due to intramolecular alkyl chain flexibility.

It is rather surprising to notice that the cone angle is larger than 45° in most cases. In DPPC and DSPC membranes in particular, the cone angle is larger than 45° for all temperatures above the phase-transition temperature. This result indicates that restriction on CSL wobbling imposed by the environment is not very strict in these PC membranes above

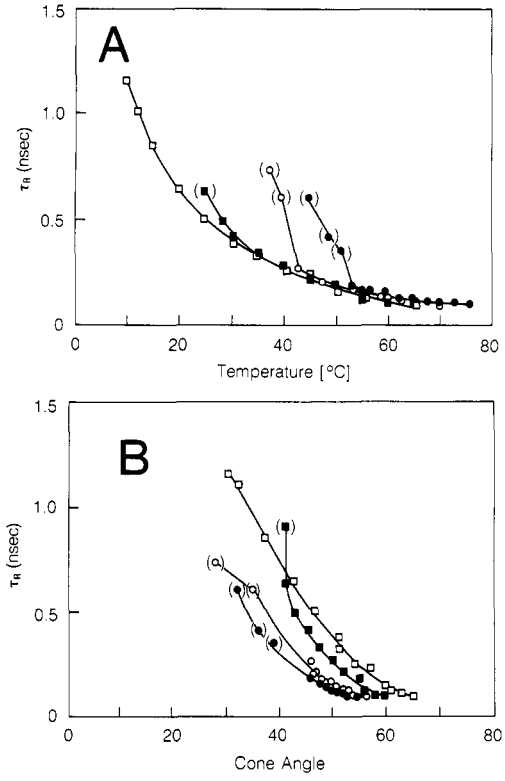

FIGURE 5: (A) τ_R plotted against temperature. (B) τ_R plotted against cone angle. (□) DLPC; (■) DMPC; (○) DPPC; (●) DSPC.

the phase-transition temperatures. This agrees well with the conclusion by Merkle et al. (1987), who found a large collision rate of lipid alkyl chains with a molecule located on the membrane surface.

τ_R is plotted against temperature in Figure 5A. τ_R is a mixed correlation time of CSL rotation about its long axis and wobbling of the long axis of CSL itself (Israelachvili et al., 1975). In Figure 5A, all points follow almost the same curve above the phase-transition temperatures for the host phospholipid membranes. Since τ_R is a function of the cone angle (eq 3), τ_R for CSL in different host lipid membranes can be directly compared only when the cone angles are the same. For this purpose, τ_R is plotted against the cone angle in Figure 5B. Figure 5B shows that τ_R is *longer* in the PC membrane with *shorter* alkyl chains if τ_R is compared at the same cone angle. This is not simply due to the fact that, for longer chains, the same cone angle is obtained at higher temperatures because when $\tau_R kT$ is plotted against the cone angle, the plot shows the same tendency as in Figure 5B (results not shown). These results clearly indicate that the cone angle, a measure of the restoring potential, and the viscosity inside the cone are affected by different factors and/or mechanisms. They also indicate that the motion of lipid in different membranes may be very different even if the order parameters (cone angles) are the same. In most spectroscopic studies of lipid motion in membranes, including ESR, NMR, and steady-state fluorescence, the key parameter investigated is the order parameter. Not much attention has been paid to the rotational diffusion rate of the probe or viscosity "felt" by the probe (Kintanar et al., 1986, and references therein). The results displayed in Figure 5 indicate that both the rotational diffusion rate inside the cone and the restoring potential imposed by the environment are significant in describing the probe motion.

In Figure 6, τ_w, the rotational correlation time of the CSL long axis itself (wobbling), is plotted against temperature. Since τ_w depends on both cone angle and D_w (eq 3 and 6), its temperature dependence is complex. τ_w becomes shorter for

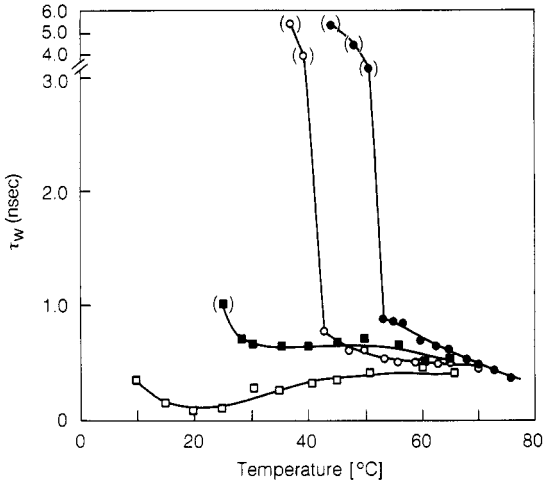

FIGURE 6: τ_w plotted against temperature. Symbols are the same as those for previous figures.

the same D_w as the cone angle decreases. D_w and the cone angle are the only two independent parameters that describe Brownian diffusion of CSL within the confines of a cone. D_w can be calculated from τ_w and the cone angle by using eq 6. D_w is plotted against inverse temperature in Figure 7. The Arrhenius plots of D_w show straight lines above the phase-transition temperature of each phospholipid membrane. D_w decreases as the chain length increases in saturated PC membranes if D_w's are compared at the same temperature. D_w of CSL in DOPC membranes is plotted for comparison in Figure 7A.

The activation energy for wobbling diffusion was estimated from Figure 7 and is shown in Table II together with the activation energy for lateral diffusion of phospholipids obtained from NMR measurements (Kuo & Wade, 1979). Activation energy for CSL wobbling increases as the chain length increases in saturated PC membranes. It is smaller than the activation energy for translational diffusion of phospholipid in these membranes. (The activation energy for wobbling diffusion in DOPC membranes can be compared with that for translational diffusion in egg-yolk PC membranes.) In contrast to the observation that the rotational diffusion of rhodopsin about the bilayer normal does not depend on the chain length in lipid-rich reconstituted membranes (Kusumi & Hyde, 1982), the wobbling diffusion of CSL is strongly dependent on the length of alkyl chains.

Table II: Activation Energy for Rotational Diffusion of CSL and Lateral Diffusion of Phospholipids in Various PC (−Cholesterol) Membranes

host lipid	ΔE for D_w (kcal/mol)	ΔE for lateral diffusion[c] (kcal/mol)
DLPC	very small	9.4 ± 0.2
DMPC	4.10 ± 0.14	15.2 ± 0.3
DPPC	6.42 ± 0.10	15.2 ± 1.3
DSPC	12.04 ± 0.14	ND[d]
EYPC[a]	ND[d]	9.0 ± 0.4
DOPC	6.48 ± 0.07	ND[d]
DOPC/chol[b] = 3/1	3.06 ± 0.11	ND[d]
DOPC/chol[b] = 1/1	2.25 ± 0.06	ND[d]

[a] Egg-yolk phosphatidylcholine. [b] chol indicates cholesterol. [c] According to Kuo and Wade (1979). [d] ND = not determined.

Effects of Cholesterol on CSL Motion in DOPC–Cholesterol Membranes. Similar experiments and analysis were carried out to study DOPC and DOPC–cholesterol membranes (molar ratios 3:1 and 1:1). The temperature dependence of the cone angle is shown in Figure 4B. If compared at the same temperature, the cone angles for CSL in DOPC membranes are between those for DLPC and DMPC membranes. The cone angle for DOPC/cholesterol = 3/1 membranes is similar to that for DPPC membranes. The cone angle for DOPC/cholesterol = 1/1 membranes is much smaller than that for any of the saturated PC membranes.

D_w for CSL in DOPC (−cholesterol) membranes is plotted against inverse temperature in Figure 7B. D_w becomes less sensitive to a change in temperature in the presence of cholesterol. Activation energy for D_w is summarized in Table II.

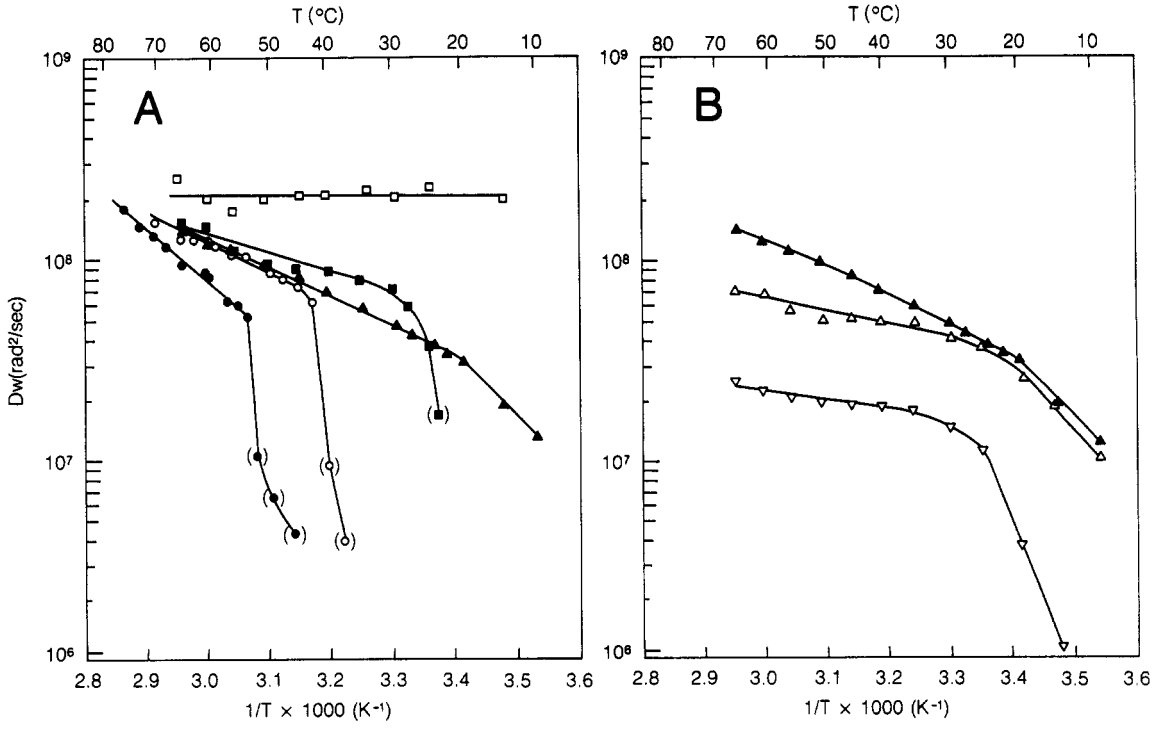

FIGURE 7: D_w plotted against T^{-1} in saturated PC (A) and DOPC–cholesterol (B) membranes. Symbols are the same as in Figure 4.

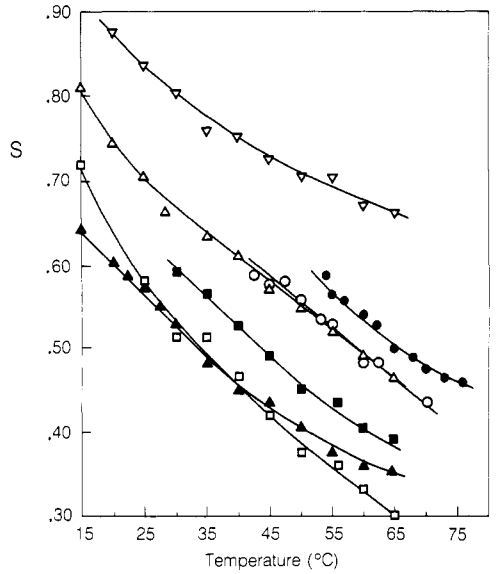

FIGURE 8: Order parameter (S) plotted against temperature. Symbols are the same as in previous figures.

Both the diffusion constant and the activation energy for wobbling diffusion of CSL in DOPC membranes are between those in DMPC and DPPC membranes. A large decrease of activation energy is observed when cholesterol is incorporated in DOPC membranes. These results are qualitatively in agreement with previous data showing that cholesterol diminishes the temperature dependence of dynamic properties of membranes (Gally et al., 1976; Rice et al., 1979).

General Discussion. We have made systematic studies on rotational diffusion of a rigid sterol molecule, CSL, in various PC membranes as a function of alkyl chain length, unsaturation, cholesterol content, and temperature. By simulating steady-state ESR spectra of CSL in the membrane, we were able to estimate the cone angle (Figure 4), the wobbling diffusion constant (Figure 7), and the activation energy for wobbling diffusion (Table II) for CSL. The order parameter S (eq 1) can be calculated from the cone angle by assuming homogeneous distribution of the orientations of CSL long axis in the cone:[2]

$$S = \int_0^{\theta_c}(3\cos^2\theta - 1)/2 \sin\theta\, d\theta / \int_0^{\theta_c}\sin\theta\, d\theta = \tfrac{1}{2}\cos\theta_c(1 + \cos\theta_c) \quad (7)$$

S is plotted against temperature in Figure 8. The temperature profile of S for DOPC membranes is similar to that for DLPC. This indicates a large influence of a cis double bond (between the 9th and 10th carbons) in the alkyl chain of the host lipid on the order of CSL long axis. This result is apparently at variance with our previous observation, in which a cis double bond in an alkyl chain gives only a minor effect on gauche–trans isomerization in stearic acid spin-labels (Kusumi et al., 1986). It is concluded that unsaturation in an alkyl chain affects the motion of rigid molecules such as cholesterol in the membrane, while it gives much smaller effects on gauche–trans isomerization. The temperature profile of S for DOPC/cholesterol = 3/1 membranes shows a large effect of cholesterol on CSL motion in DOPC membranes, and it is similar to that for DPPC above the phase-transition temperature. We previously observed that unsaturation of alkyl chains moderates the effect of cholesterol on motional freedom of 5- and 16-doxylstearic acid spin-labels. The motion of rigid molecules as a whole can be influenced by almost any changes in interaction with surrounding molecules. In flexible molecules, the local effect from the surrounding environment might not be transmitted to other parts of the molecule. The mobility of rigid sterol molecules as a whole in the membrane can be much susceptible to changes in cholesterol content and the degree of alkyl chain unsaturation than the alkyl chain flexibility.

[2] The order parameter used here is based on the common definition for an axially symmetric probe in uniaxial medium

$$S = \tfrac{1}{2}(3\cos^2\theta - 1)_{av} = \langle D^2_{00}(\Omega)\rangle = \frac{\int d\Omega \exp(-U/kT) D^2_{00}(\Omega)}{\int d\Omega \exp(-U/kT)}$$

where U is the mean orienting potential, $D^2_{00}(\Omega)$ is an element of the Wigner rotation matrix of rank 2, and θ (Ω) is the (Euler) angle between the molecular ordering and the symmetric axis of the molecule.

Table III: Comparison of Motional Parameters of Various Probes in PC–Cholesterol Membranes

host lipid	temp (°C)	probe	D_w ($\times 10^7$ s^{-1})	θ_c (deg)	S
DMPC	35	CSL	7.0	47.5	0.57
DMPC[a]	35	ASL[g]	8.7	64.2	0.31
DMPC[b]	35	DPH[h]	15.6	61.8	0.34
DPPC	50	CSL	7.7	48.0	0.55
DPPC[a]	50	ASL[g]	11.4	66.0	0.28
DPPC[c]	50	DPH[h]	29.0	60.9	0.36
DPPC/chol = 1/1[d,e]	49	CSL	0.34	25	0.86
DOPC/chol = 75/25	30	CSL	4.5	41	0.66
EYPC/chol = 70/30[d,f]	30	^{2}H-chol			0.75
DOPC/chol = 1/1[d]	30	CSL	1.4	31	0.80
EYPC/chol = 1/1[d,f]	30	^{2}H-chol			0.80

[a] From Pasenkiewicz et al. (1987). [b] From Kinosita and Ikegami (1984). [c] From Kinosita et al. (1984). [d] chol indicates cholesterol. [e] From Hemminga (1974). [f] From Taylor et al. (1982). [g] ASL = androstane spin-label. [h] DPH = 1,6-diphenyl-1,3,5-hexatriene.

D_w, θ_c, and S obtained for different probes are compared in Table III (Hemminga, 1974; Stubbs et al., 1981; Taylor et al., 1982; Kinosita & Ikegami, 1984; Kinosita et al., 1984; M. Pasenkiewicz-Gierula, W. K. Subczynski, and A. Kusumi, unpublished results). When comparing CSL data with the results of androstane spin-label, another spin-labeled sterol analogue, one notices larger D_w and θ_c for androstane spin-label. This result indicates that androstane spin-label may be localized in a more central region of the membrane than CSL where it experiences more motional freedom. Hemminga (1974) analyzed CSL motion in DPPC/cholesterol = 1/1 membranes by using a different simulation method. Comparison of his data and our results indicates that cholesterol greatly decreases both D_w and θ_c.

The S-value determined for cholesterol by NMR method (Taylor et al., 1982) agrees with that for CSL in unsaturated PC membranes containing 50 mol % cholesterol, while it is larger than S for CSL in the presence of 25–30 mol % cholesterol (Table III). The lack of a 3-β-OH group in CSL and/or a difference in the definition of orienting potential may explain this difference.

Kinosita et al. (1983) and Kinosita and Ikegami (1984) estimated D_w and θ_c from time-resolved fluorescence anisotropy decays of 1,6-diphenyl-1,3,5-hexatriene (DPH) in various PC membranes (Table III). DPH motion in the membrane can also be analyzed as a rigid rod undergoing Brownian rotational diffusion in a cone. θ_c values for DPH in DMPC and DPPC membranes are similar to those for androstane spin-label and larger than those for CSL. D_w values are larger by a factor

of 2–4 than for CSL and androstane spin-label. Since DPH is expected to localize in the middle of the bilayer and since the molecule is less bulky than CSL or androstane spin-label, greater mobility of DPH seems to be reasonable. The use of spin probes in membrane studies can be more advantageous than DPH because (1) experimental and analysis time required for CSL studies is much shorter than that for time-resolved fluorescence anisotropy studies of DPH (steady-state fluorescence experiments cannot evaluate both D_w and θ_c) and (2) the structure of CSL resembles the structure of cholesterol, while DPH has no structural similarity to any membrane component.

It is found that the cone angle, D_w, and the activation energy for D_w are strongly dependent on alkyl chain length, unsaturation, and cholesterol content in the membrane. Activation energy for wobbling diffusion depends on alkyl chain length and unsaturation more than that for translational diffusion (Table II). The former is smaller than the latter.

The presence of 50 mol % cholesterol in DOPC membranes decreases the activation energy for wobbling diffusion by a factor of 3. On the other hand, it decreases D_w by a factor of about 3–6. These results are probably due to a complex interplay of decreased jump distance and increased jump rate of CSL induced by cholesterol.

In spin-label studies of membranes, CSL and androstane spin-label have been widely used as analogues for cholesterol (Presti & Chan, 1982; Presti et al., 1982). In the present paper, we report on CSL motion with special attention paid to the wobbling diffusion constant, which can be related to the viscosity (inside the cone) arising from the interaction between CSL and surrounding lipids, and its activation energy. We chose CSL rather than androstane spin-label because its molecular structure is closer to that of cholesterol. Nevertheless, CSL cannot be expected to mimic all properties of cholesterol because of the lack of a 3-β-OH group. However, overall similarity of the phase behavior of PC–CSL membranes and PC–cholesterol membranes has been reported (Cadenhead & Müller-Landau, 1979). Thus, dynamic behavior of CSL reported in this paper should approximate cholesterol–PC and cholesterol–cholesterol interactions in the membrane.

Conclusion

(1) Magnetic parameters for CSL in various PC and PC–cholesterol membranes have been determined from Q-band ESR spectra at −120 °C. These values are used for simulating ESR spectra of CSL in these membranes at physiological temperatures. It is concluded that magnetic parameters determined at −120 °C are close to those in unfrozen samples and that water accessibility to the membrane surface increases with increase in cholesterol mole fraction in the membrane.

(2) Wobbling diffusion constants were obtained in various phosphatidylcholine membranes, and the activation energies for the diffusion were determined from the Arrhenius plots of the diffusion constants.

(3) Activation energy for D_w increases in the order DLPC < DOPC/cholesterol = 1/1 < DOPC/cholesterol = 3/1 < DMPC < DOPC ~ DPPC < DSPC.

(4) D_w decreases in the order DLPC > DMPC > DOPC ~ DPPC > DSPC > DOPC/cholesterol = 3/1 > DOPC/cholesterol = 1/1 when D_w's are compared at the same temperature.

(5) The cone angle decreases in the order DLPC > DOPC > DMPC > DOPC/cholesterol = 3/1 > DPPC > DSPC ≫ DOPC/cholesterol = 1/1.

(6) The activation energy for wobbling diffusion of CSL in PC membranes is smaller than the activation energy for translational diffusion of a phospholipid. The former is more dependent on alkyl chain length and unsaturation.

Acknowledgments

We thank Dr. James S. Hyde at the Medical College of Wisconsin and Dr. S. Ohnishi at Kyoto University for helpful discussion and support. We are grateful to Dr. B. Hudson at Carroll College for critical reading of the manuscript.

References

Arderle, G., & Mendelsohn, R. (1986) *Biochemistry 25*, 2174–2179.

Blumenthal, R., Seth, P., Willingham, M. C., & Pastan, I. (1986) *Biochemistry 25*, 2231–2237.

Borg, D. C. (1972) in *Biological Applications of Electron Spin Resonance* (Schwartz, H. M., Bolton, J. R., & Borg, D. C., Eds.) p 100, Wiley, New York.

Cadenhead, D. A., & Müller-Landau, F. (1979) *Chem. Phys. Lipids 25*, 329–343.

Dempsey, C. E., Ryba, N. J. P., & Watts, A. (1986) *Biochemistry 25*, 2180–2187.

Dufourc, E. J., & Smith, I. C. P. (1986) *Chem. Phys. Lipids 41*, 123–135.

Engel, L. W., & Prendergast, F. G. (1981) *Biochemistry 20*, 7338–7345.

Gally, H. U., Seelig, A., & Sellig, J. (1976) *Hoppe-Seyler's Z. Physiol. Chem. 357*, 1447–1450.

Goldman, S. A., Bruno, G. V., Polnaszek, C. F., & Freed, J. H. (1972) *J. Chem. Phys. 56*, 716–735.

Griffith, O. H., & Jost, P. (1976) in *Spin Labeling, Theory and Applications* (Berliner, L. J., Ed.) Chapter 12, pp 453–525, Academic, New York.

Hemminga, M. A. (1974) *Chem. Phys. 6*, 87–99.

Hemminga, M. A. (1977) *J. Magn. Reson. 25*, 25–45.

Hubbell, W. L., & McConnell, H. M. (1971) *J. Am. Chem. Soc. 93*, 314–326.

Israelachvili, J., Sjosten, J., Ericksson, L. E. G., Ehrstrom, J., Graslund, A., & Ehrenberg, A. (1975) *Biochim. Biophys. Acta 382*, 125–141.

Jost, P. C., & Griffith, O. H. (1973) *Arch. Biochem. Biophys. 159*, 70–76.

Kawato, S., Kinosita, K., Jr., & Ikegami, A. (1977) *Biochemistry 16*, 2319–2324.

Kawato, S., Kinosita, K., Jr., & Ikegami, A. (1978) *Biochemistry 17*, 5029–5031.

Kinosita, K., Jr., & Ikegami, A. (1984) *Biochim. Biophys. Acta 769*, 523–527.

Kinosita, K., Jr., Kawato, S., & Ikegami, A. (1977) *Biophys. J. 20*, 289–305.

Kinosita, K., Jr., Kawato, S., & Ikegami, A. (1984) *Adv. Biophys. 17*, 147–203.

Kintanar, A., Kunwar, A. C., & Oldfield, E. (1986) *Biochemistry 25*, 6517–6524.

Kuo, A.-L., & Wade, C. G. (1979) *Biochemistry 18*, 2300–2308.

Kusumi, A., & Hyde, J. S. (1982) *Biochemistry 21*, 5978–5983.

Kusumi, A., Ohnishi, S., Ito, T., & Yoshizawa, T. (1978) *Biochim. Biophys. Acta 507*, 539–543.

Kusumi, A., Sakaki, T., Yoshizawa, T., & Ohnishi, S. (1980) *J. Biochem. (Tokyo) 88*, 1103–1111.

Kusumi, A., Subczynski, W. K., & Hyde, J. S. (1982) *Proc. Natl. Acad. Sci. U.S.A. 79*, 1854–1858.

Kusumi, A., Subczynski, W. K., Pasenkiewicz-Gierula, M., Hyde, J. S., & Merkle, H. (1986) *Biochim. Biophys. Acta 854*, 307–317.

Madden, K., Kevan, L., Morse, P. D., & Schwartz, R. (1980) *J. Phys. Chem. 84*, 2691–2692.
Mailer, C., Taylor, C. P. S., Schreier-Muccillo, S., & Smith, I. C. P. (1974) *Arch. Biochem. Biophys. 159*, 133–144.
McConnell, H. M. (1976) in *Spin Labeling, Theory and Applications* (Berliner, L. J., Ed.) pp 525–560, Academic, New York.
Meirovitch, E., & Freed, J. H. (1984) *J. Phys. Chem. 88*, 4995–5004.
Merkle, H., Subczynski, W. K., & Kusumi, A. (1987) *Biochim. Biophys. Acta 897*, 238–248.
Müller-Landau, F., & Cadenhead, D. A. (1979a) *Chem. Phys. Lipids 25*, 299–314.
Müller-Landau, F., & Cadenhead, D. A. (1979b) *Chem. Phys. Lipids 25*, 315–328.
Nordio, P. L., & Busolin, P. (1971) *J. Chem. Phys. 55*, 5485–5490.
Pal, B. (1918) *Bull. Calcutta Math. Soc. 9*, 85–95.
Parente, R. A., & Lentz, B. R. (1986) *Biochemistry 25*, 6678–6688.
Pasenkiewicz-Gierula, M., Hyde, J. S., & Pilbrow, J. R. (1983) *J. Magn. Reson. 55*, 255–265.
Polnaszek, C. F., Bruno, G. V., & Freed, J. H. (1973) *J. Chem. Phys. 58*, 3185–3199.
Polnaszek, C. F., Marsh, D., & Smith, I. C. P. (1981) *J. Magn. Reson. 43*, 54–64.
Popp, C. A., & Hyde, J. S. (1981) *J. Magn. Reson. 43*, 249–258.
Presti, F. T., & Chan, S.-I. (1982) *Biochemistry 21*, 3821–3830.
Presti, F. T., Pace, R. J., & Chan, S.-I. (1982) *Biochemistry 21*, 3831–3835.
Rao, K. V. S., Polnaszek, C. F., & Freed, J. H. (1977) *J. Phys. Chem. 81*, 449–456.
Rice, D. M., Meadows, M. D., Scheinman, A. O., Goni, F. M., Gomez-Fernandez, J. C., Schreier, S., Polnaszek, C. F., & Smith, I. C. P. (1978) *Biochim. Biophys. Acta 515*, 375–436.
Schindler, H., & Seelig, J. (1973) *J. Chem. Phys. 59*, 1841–1850.
Schindler, H., & Seelig, J. (1974) *J. Chem. Phys. 61*, 2946–2949.
Shimoyama, Y., Eriksson, L. E. G., & Ehrenberg, A. (1978) *Biochim. Biophys. Acta 508*, 213–235.
Stubbs, C. D., Kouyama, T., Kinosita, K., Jr., & Ikegami, A. (1981) *Biochemistry 20*, 4257–4262.
Subczynski, W. K., Antholine, W. E., Hyde, J. S., & Petering, D. H. (1987) *J. Am. Chem. Soc. 109*, 46–52.
Taylor, M. G., Akiyama, T., Saito, H., & Smith, I. C. P. (1982) *Chem. Phys. Lipids 31*, 359–379.
Wang, C. C., & Pecora, R. (1980) *J. Chem. Phys. 72*, 5333–5340.

Biosynthesis of the 2-(Aminomethyl)-4-(hydroxymethyl)furan Subunit of Methanofuran†

Robert H. White
Department of Biochemistry and Nutrition, Virginia Polytechnic Institute and State University, Blacksburg, Virginia 24061
Received October 14, 1987; Revised Manuscript Received January 8, 1988

ABSTRACT: ^{2}H- and ^{13}C-labeled precursors were used to establish the pathway for the biosynthesis of the 2-(aminomethyl)-4-(hydroxymethyl)furan (F1) component of methanofuran in methanogenic archaebacteria. The extent and position of the label incorporated into F1 were measured from the mass spectrum of the diacetyl derivative of F1. [1,2-$^{13}C_2$]Acetate was found to be incorporated into two separate positions of the F1 molecule as a unit. The extent of incorporation of $^{13}C_2$ into each of these positions was the same as that observed for the incorporation of acetate into the alanine and proline produced by the cells. From [2,2,2-$^{2}H_3$]acetate, deuterium was incorporated into two separate sites of the F1 molecule, one containing up to two deuteriums and the other only one. On the basis of the fragmentation pattern of the F1 diacetyl derivative, it was determined that two deuteriums were incorporated into the hydroxymethyl group at C-4 and one was incorporated at C-3 of the furan ring. The extent and distribution of the incorporated deuterium at the C-4 methylene were the same as that observed for C-6 of the glucose produced by the cells. On the basis of this and additional information presented in this paper, it is concluded that F1 is generated by the condensation of dihydroxyacetone phosphate with pyruvate. The resulting dihydroxy-substituted tetrahydrofuran after elimination of 2 mol of water would produce the phosphate ester of 2-carboxy-4-(hydroxymethyl)furan. Reduction of the carboxylic acid to an aldehyde and subsequent transamination would produce the phosphate ester of F1.

Natural products containing a furan ring have been isolated from a large number of different organisms. These furans can be classified into three major structural types: the furanoterpenoids, which can contain mono-, di-, and trisubstituted furan ring(s) (Hikino & Konno, 1976; Sullivan et al., 1983); the furanocoumarins, in which the C-2 and C-3 carbons of the furan are shared by an aromatic ring (Floss & Mothes, 1966; Games & James, 1972); and the fatty acid derived furans, which are generally 2,5-disubstituted furans (Morris et al., 1966; Rahn et al. 1979; Sand et al., 1983; Rau et al., 1984). On the basis of the structures of these furans and a limited number of labeling experiments (Hikino & Konno, 1976), it is concluded that the first two classes of furans are terpene derived and that the latter is fatty acid derived. None of these

†This work was funded by National Science Foundation Grant PCM-8217072 and is the second in a series of papers on the biosynthesis of the subunits of methanofuran.

0006-2960/88/0427-4415$01.50/0